Molecular Cell
Article

Ultrasensitivity in the Regulation of Cdc25C by Cdk1

Nicole B. Trunnell,[1,2] Andy C. Poon,[1] Sun Young Kim,[1] and James E. Ferrell, Jr.[1,3,*]
[1]Department of Chemical and Systems Biology
[2]Program in Cancer Biology
[3]Department of Biochemistry
Stanford University School of Medicine, Stanford, CA 94305-5174, USA
*Correspondence: james.ferrell@stanford.edu
DOI 10.1016/j.molcel.2011.01.012

SUMMARY

Cdc25C is a critical component of the interlinked positive and double-negative feedback loops that constitute the bistable mitotic trigger. Computational studies have indicated that the trigger's bistability should be more robust if the individual legs of the loops exhibit ultrasensitive responses. Here, we show that in *Xenopus* extracts two measures of Cdc25C activation (hyperphosphorylation and Ser 287 dephosphorylation) are highly ultrasensitive functions of the Cdk1 activity; estimated Hill coefficients were 11 to 32. Some of Cdc25C's ultrasensitivity can be reconstituted in vitro with purified components, and the reconstituted ultrasensitivity depends upon multisite phosphorylation. The response functions determined here for Cdc25C and previously for Wee1A allow us to formulate a simple mathematical model of the transition between interphase and mitosis. The model shows how the continuously variable regulators of mitosis work collectively to generate a switch-like, hysteretic response.

INTRODUCTION

In eukaryotes, mitosis is driven by the cyclin B1-Cdk1 complex (Morgan, 2007). The enzymatic activity of cyclin B1-Cdk1 depends upon the phosphorylation state of Cdk1: a conserved threonine residue in the activation loop (Thr 161 in human and *Xenopus laevis* Cdk1) must be phosphorylated, and two sites in the ATP binding pocket (Thr 14 and Tyr 15 in human and *Xenopus* Cdk1) must be dephosphorylated. Kinases of the Wee1/Myt1 family phosphorylate Thr 14 and Tyr 15 (Booher et al., 1997; Fattaey and Booher, 1997; Heald et al., 1993; Liu et al., 1997; McGowan and Russell, 1993; Mueller et al., 1995b; Parker and Piwnica-Worms, 1992). Phosphatases of the Cdc25 family dephosphorylate both of these sites (Millar et al., 1991; Strausfeld et al., 1991). Thus, Cdc25 is an activator of Cdk1, and Wee1 and Myt1 are inactivators.

Wee1 and Cdc25 not only regulate Cdk1, they are also regulated in turn by Cdk1. The same is true of the less-studied Myt1 protein (Booher et al., 1997; Fattaey and Booher, 1997; Liu et al., 1997; Mueller et al., 1995b; Palmer et al., 1998); for simplicity, we focus here on Wee1 and Cdc25. Cdk1 phosphorylates and activates Cdc25 (Hoffmann et al., 1993; Kumagai and Dunphy, 1992; Solomon et al., 1990), and it phosphorylates and inhibits Wee1 (McGowan and Russell, 1995; Mueller et al., 1995a; Mueller et al., 1995b). Thus, the Cdk1/Wee1/Cdc25 system can be viewed as two interlocking, mirror-image feedback loops: a double-negative feedback loop (Wee1 –| Cdk1 –| Wee1) and a positive feedback loop (Cdc25 → Cdk1 → Cdc25). Early theoretical work (Novak and Tyson, 1993a, b; Thron, 1996) proposed that these feedback loops constitute a bistable mitotic trigger that could account for the observed temporal abruptness of Cdk1 activation and the all-or-none character of the transition into mitosis (Solomon et al., 1990). Biochemical studies in *Xenopus* egg extracts have shown that this is in fact the case (Pomerening et al., 2003; Sha et al., 2003). Moreover, compromising the positive feedback loops impairs the ability of *Xenopus* extracts to maintain sustained cycling (Pomerening et al., 2005) and causes severe dysregulation of the somatic cell cycle, as well (Pomerening et al., 2008). Thus, the Cdk1 system possesses an evolutionarily conserved bistable trigger, and this trigger is critical for normal cycling.

Bistability is not an inevitable consequence of positive feedback and/or double-negative feedback loops; it also depends upon the shapes of the steady-state response functions for each step in each the loop (e.g., the stimulus/response relationship for Cdc25 activity as a function of Cdk1 activity in the absence of feedback) and the balance between the activation and inactivation rates. In particular, ultrasensitive response functions—sigmoidal stimulus/response relationships resembling those of cooperative enzymes—facilitate the generation of bistability (Ferrell, 2008; Ferrell and Xiong, 2001). Accordingly, models of the mitotic oscillator generally assume that some sort of mechanism contributes ultrasensitivity to the Wee1 and/or Cdc25 responses (Novak and Tyson, 1993a, 1993b; Thron, 1994, 1996).

Given the importance of bistability for mitotic oscillations (Pomerening et al., 2005, 2008) and the importance of ultrasensitivity for generating a bistable response (Ferrell and Xiong, 2001), we have been exploring the question of which components of the Cdk1/Cdc25/Wee1 system exhibit ultrasensitive responses, and what mechanisms underpin any ultrasensitivity

we find. Cooperativity is probably the most familiar mechanism for generating an ultrasensitive response, but there are several others, and it is not clear which of these mechanisms are the most important or most common in biological regulation. Recently, we showed that in *Xenopus* egg extracts, the phosphorylation of Wee1A by Cdk1 in the absence of feedback is highly ultrasensitive, with an apparent Hill coefficient of 3 to 4, and proposed that this ultrasensitivity was generated by a combination of multisite phosphorylation and competition (Kim and Ferrell, 2007). In principle, this ultrasensitivity could be sufficient to generate bistability in the Cdk1/Cdc25/Wee1 system. However, an additional ultrasensitive response in the regulation of Cdc25 would be expected to substantially improve the robustness of the bistable Cdk1/Cdc25/Wee1 system (Ferrell, 2008). This motivated the present study, in which we set out to determine whether the steady-state response of Cdc25 to Cdk1 was ultrasensitive and what mechanisms underpinned any ultrasensitivity observed.

In most vertebrate species there are three isoforms of Cdc25: Cdc25A, Cdc25B, and Cdc25C. These phosphatases share a relatively well-conserved C-terminal catalytic domain that is a member of the rhodanese family of folds, a different fold from those found in other phosphoprotein phosphatases (Fauman et al., 1998). The N-terminal half of the Cdc25 proteins is less well conserved and functions as a regulatory domain. The three Cdc25 genes are thought to play overlapping roles in cell cycle regulation. Cdc25A is essential in early embryonic development in mice (Lee et al., 2009), whereas Cdc25B and Cdc25C are not (Ferguson et al., 2005). In adult mice, none of the three Cdc25 isoforms is individually essential, but knocking out all three causes death due to loss of rapidly proliferating epithelial cells (Lee et al., 2009). Here, we chose to focus on the regulation of the *Xenopus* Cdc25C protein because of the powerful tools available for quantitative biochemical studies in the *Xenopus* system and because immunodepletion studies have indicated that Cdc25C is essential for mitosis in *Xenopus* extracts (Izumi and Maller, 1993).

The N terminus of Cdc25C becomes highly phosphorylated during mitosis (Izumi and Maller, 1993; Kumagai and Dunphy, 1992), resulting in a shift in the apparent molecular mass of the protein from 70 kDa to 100 kDa on immunoblots. There are 14 SP and TP sites in the N terminus of *Xenopus* Cdc25C, of which at least five are phosphorylated in mitosis (T48, T67, T138, S205, and S285) (Izumi and Maller, 1993). Cdk1 and other proline-directed kinases (such as p42 MAPK [Wang et al., 2007]) are probably responsible for these SP/TP phosphorylations. Cdc25C is phosphorylated on multiple other sites by Polo-like kinase-1 (termed Plx1 in *Xenopus*) (Kumagai and Dunphy, 1996). Polo-like kinases have been shown to preferentially bind phosphorylated residues (Elia et al., 2003), raising the possibility that Cdk1 phosphorylation primes Cdc25 for phosphorylation by Plx1.

Cdc25C may also be regulated by prolyl *cis-trans* isomerization. Mitotic Cdc25C binds to Pin1, a prolyl isomerase with affinity for phosphorylated residues (Shen et al., 1998). This may result in a change in the conformation of Cdc25C (Stukenberg and Kirschner, 2001), a change in the rate of dephosphorylation of Cdc25C (Zhou et al., 2000), or both.

The net effect of these various phosphorylations and isomerizations is that Cdc25C increases in activity at the onset of mitosis (Izumi et al., 1992; Kumagai and Dunphy, 1992) and accumulates at the centrosome and in the nucleus (Bonnet et al., 2008; Kumagai and Dunphy, 1999; Lopez-Girona et al., 1999, 2001; Toyoshima-Morimoto et al., 2002).

Cdc25C is also phosphorylated during interphase. Whereas the mitotic phosphorylations are associated with activation of Cdc25C, the interphase phosphorylation of Ser 287 (*Xenopus* numbering) results in the cytoplasmic sequestration and functional inactivation of Cdc25C by 14-3-3 proteins (Kumagai and Dunphy, 1999; Lopez-Girona et al., 1999). The protein kinases Chk1, Chk2, MAPKAP kinase-2 (MK2), and TAK1 have been implicated in Ser 287 phosphorylation (Furnari et al., 1997; Manke et al., 2005; Matsuoka et al., 1998; Matsuoka et al., 2000; Peng et al., 1998; Sanchez et al., 1997).

Given the complexities of Cdc25C regulation, the Cdc25C responses we have chosen to focus on are Cdc25C hyperphosphorylation and Cdc25C Ser 287 dephosphorylation, for several reasons. First, both responses are easy to measure in cell-free egg extracts, whereas Cdc25C activity assays proved to be poorly reproducible for reasons we do not completely understand. Second, all of the putative endpoints of Cdc25C regulation—activation, conformation changes, and relocalization to the nucleus—are thought to depend upon Cdc25C hyperphosphorylation and Ser 287 dephosphorylation. Finally, both responses correlate reliably with mitosis as assessed by DAPI-staining of sperm chromatin in extracts. Thus, we set out to determine how the steady-state level of Cdc25C phosphorylation depends upon Cdk1 activity. We show that the response of Cdc25C to Cdk1 is highly ultrasensitive and that some of this ultrasensitivity is due to multisite phosphorylation. We also delineate the classes of mechanism through which multisite phosphorylation can generate ultrasensitivity and formulate a simple model to account for the robust bistability of the mitotic trigger.

RESULTS

Ultrasensitivity Cdc25C Responses in *Xenopus* Extracts

We set out to determine how the steady-state level of Cdc25C phosphorylation varies with the activity of Cdk1. Normally, Cdk1 activates Cdc25C and Cdc25C feeds back to activate Cdk1, making it difficult to obtain intermediate levels of either Cdc25C phosphorylation or Cdk1 activity. Without data on these intermediate responses, it would be difficult to judge the precise shape of the Cdc25C response function.

To circumvent this problem, we made use of a phosphorylation site mutant of Cdk1, Cdk1-T14A/Y15F (Cdk1AF), which cannot be inactivated by Wee1 or Myt1 and need not be activated by Cdc25 (Figure 1A). We mixed purified recombinant Cdk1AF with nondegradable *Xenopus* cyclin B1 (Δ65-cyclin B1 [Pomerening et al., 2003]) and added various concentrations to cyclin-free, interphase *Xenopus* egg extracts, to yield final concentrations of 200 nM Cdk1AF and 0–130 nM Δ65-cyclin B1. The Cdk1AF-cyclin B1-supplemented extracts were incubated at room temperature for 120 min to allow them to approach a steady-state with respect to the activity of Cdk1,

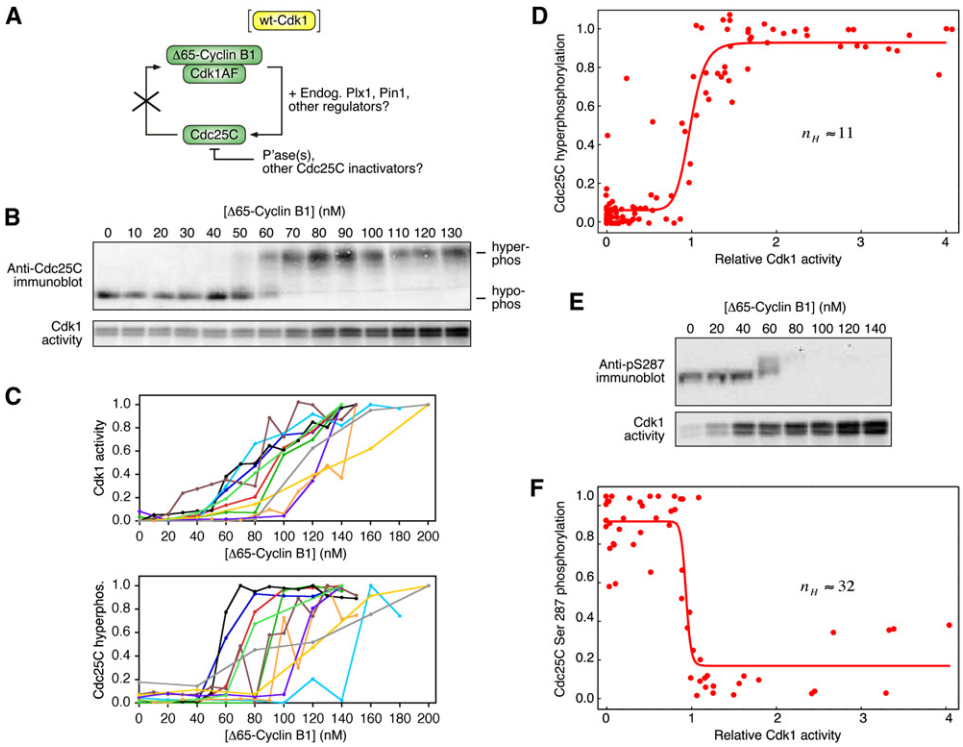

Figure 1. Ultrasensitive Hyperphosphorylation of Cdc25C in *Xenopus* Egg Extracts

(A) Endogenous Cdc25C was phosphorylated in *Xenopus* extract in response to various concentrations of Δ65-cyclin B1-Cdk1AF. The AF mutation avoids the feedback regulation of Cdk1 by Cdc25C.

(B and C) Steady-state responses of Cdk1 and Cdc25C to various concentrations of Δ65-cyclin B1-Cdk1AF. Primary data from one experiment (B) and plots of Cdk1 and Cdc25C responses from 11 experiments (C) are shown.

(D) Cdc25C hyperphosphorylation as a function of Cdk1 activity. Scaled data from 11 experiments were pooled and fitted to a four-parameter Hill function. The Hill coefficient n_H was 11. The 95% confidence interval for n_H was 6 to 17.

(E) Steady-state dephosphorylation of Cdc25C at Ser 287 (top) as assessed by immunoblotting and GelDoc quantitation, and steady-state Cdk1 activity (bottom) as assessed by histone H1 kinase assays and quantitative autoradiography.

(F) Cdc25C Ser 287 phosphorylation as a function of Cdk1 activity. Scaled data from seven data sets (four independent experiments) were pooled and fitted to a four-parameter Hill function. The Hill coefficient n_H was 32 with a 95% confidence interval of 17 to 47.

as measured by histone H1 kinase assays and quantitative autoradiography, and the hyperphosphorylation of Cdc25C, as assessed by immunoblotting and quantitation. Assuming that the Δ65-cyclin B1 does not dissociate from the Cdk1AF and bind to the endogenous Cdk1 protein, one would expect the activity of the Cdk1AF complexes to be linearly proportional to the amount of added Δ65-cyclin B1. In some experiments, this was the case, although more often the response was nonlinear (Figures 1B and 1C). Nevertheless, it was possible to achieve a range of intermediate steady-state Cdk1 activities (Figure 1C). The hyperphosphorylation of Cdc25C was found to be more switch-like than the H1 kinase activity; over a narrow range of Δ65-cyclin B1 concentrations and Cdk1 activities, the Cdc25C hyperphosphorylation increased from undetectable to maximal (Figure 1C).

To separate any nonlinearity in the response of Cdk1 to Δ65-cyclin B1 from the nonlinearity in the response of Cdc25C to Cdk1, we plotted steady-state Cdc25C hyperphosphorylation on the y axis and steady-state Cdk1 activity on the x axis. Data from 11 experiments were scaled, pooled and fitted to a four-parameter Hill equation (Figure 1D). The Hill coefficient from the pooled data was 11, with a 95% confidence interval (CI) of 6 to 17. Thus, the hyperphosphorylation of Cdc25C in *Xenopus* extracts is highly ultrasensitive.

We next asked whether the dephosphorylation of Ser 287 was switch-like or graded. As shown in Figure 1E, the steady-state level of Ser 287 phosphorylation was highly switch-like, well approximated by an inhibitory Hill function with a Hill coefficient of 32. Thus, dependence of Cdc25C on Cdk1 in *Xenopus* extracts is highly ultrasensitive as assessed both by hyperphosphorylation and by Ser 287 dephosphorylation.

Comparison of Cdc25C and Wee1A Responses

Recent work in HeLa cell extracts shows that the somatic Wee1 protein (which in *Xenopus* is termed Wee1B but in HeLa cells is termed Wee1A) is an order of magnitude more sensitive to Cdk1 activity than Cdc25 is (Deibler and Kirschner, 2010). This is proposed to result in multistep activation of Cdk1: at moderate concentrations of cyclin B1 (~55 nM), Wee1 is inactivated but Cdc25 is not yet activated, resulting in partial activation of

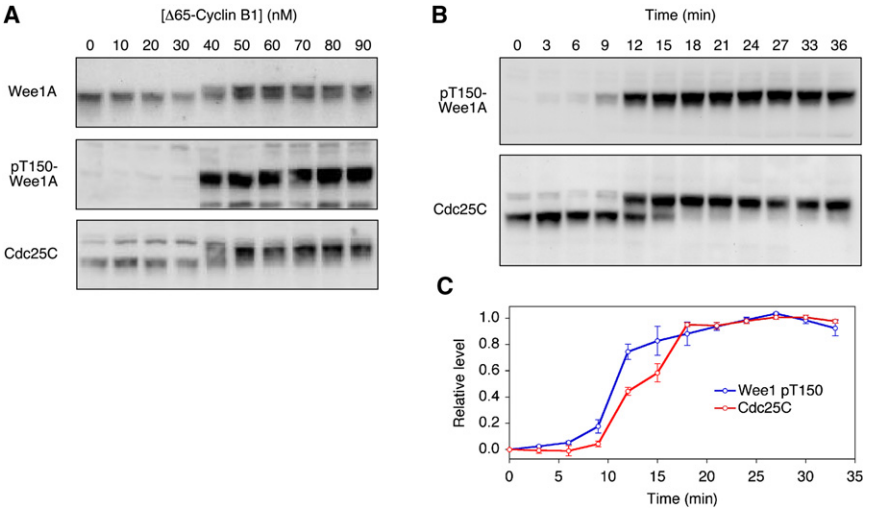

Figure 2. Comparison of Cdc25C and Wee1A Responses

(A) Steady-state responses. Extracts were incubated for 2 hr with different concentrations of nondegradable Δ65-cyclin B1, which was sufficient to allow the Wee1A and Cdc25C phosphorylation to approach steady state.

(B and C) Time courses. Extracts were incubated with 100 nM Δ65-cyclin B1 for the lengths of time indicated. (B) shows one experiment; (C) shows average results from two independent experiments. The data (C) represent means ± standard error from four replicates.

Cdk1, and only at higher concentrations (>500 nM) is Cdc25 activated (Deibler and Kirschner, 2010). The EC_{50} values measured here for *Xenopus* Cdc25C hyperphosphorylation and Cdc25C Ser 287 dephosphorylation are similar to those previously reported for *Xenopus* Wee1A hyperphosphorylation (~30–60 nM [Kim and Ferrell, 2007]). Nevertheless, batches of cyclin vary in potency, and different extracts vary in their sensitivity to cyclin, so we set out to compare the responses of Cdc25C and Wee1A more directly. As shown in Figure 2, the responses of the two proteins were nearly indistinguishable both with respect to their steady-state responses (Figure 2A) and the dynamics of their hyperphosphorylation (Figures 2B and 2C), with Wee1A perhaps requiring slightly less cyclin B1 for a full response (40 versus 50 nM; Figure 2A) and being slightly quicker in its half-maximal response (~10 versus 12 min; Figures 2B and 2C). Therefore, in this respect the *Xenopus* egg extract system appears to be different from the HeLa cell extract system; the Cdc25C and Wee1A feedback loops function together as a single switch.

Nonlinearity in the Response of Cdc25C to Cdk1 In Vitro

Given the potential complexity of Cdc25C regulation in extracts, we set out to determine whether a similar, thresholded response was also exhibited in a simpler reconstituted system. We chose to examine the phosphorylation of Cdc25C by cyclin B1-Cdk1 in the absence of feedback and dephosphorylation. For several reasons, we chose not to include a phosphatase: it is not yet clear what phosphatase (s) dephosphorylate Cdc25C in extracts, and commercially available PP2A, which we used previously as a surrogate for the Wee1 phosphatase in reconstitution studies (Kim and Ferrell, 2007), is low in purity. Moreover, omitting the phosphatase allows us to gain additional information about the sources of nonlinearity in the response of Cdc25C to Cdk1. If some of Cdc25C's ultrasensitivity were due to nonlinearity in the phosphorylation reactions, we would expect a plot of the cumulative extent of Cdc25C phosphorylation to be sigmoidal. If, however, the ultrasensitivity were solely due to nonlinearity in the dephosphorylation reactions, the phosphorylation response should not be sigmoidal.

We obtained purified Cdc25C and p13 Suc1-Δ65-cyclin B1-Cdk1AF complexes, and incubated 150 nM Cdc25C (close to its estimated endogenous concentration of 140 nM [Kumagai and Dunphy, 1992]) with various concentrations of the Cdk1AF complex and 500 μM ATP at room temperature for 1 hr. Under these conditions, the maximum level of Cdc25C hyperphosphorylation was typically about 60% as judged by immunoblotting. We plotted Cdc25C hyperphosphorylation as a function of Cdk1 activity and fitted the data to a Hill function. As shown in Figure 3, the relationship between Cdc25C hyperphosphorylation and Cdk1 activity was sigmoidal, with an apparent Hill coefficient of 2.3 (95% CI of 1.9 to 2.7). This supports the hypothesis that at least some of the nonlinearity in the Cdc25C response seen in extracts arises out of the mechanism of phosphorylation.

We hypothesized that the nonlinearity seen in vitro might be a consequence of multisite phosphorylation. To test this idea, we examined the phosphorylation of a 200 amino acid N-terminal

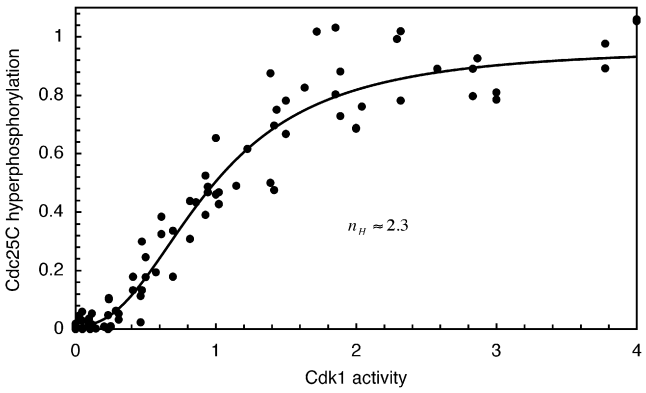

Figure 3. A Nonlinear Response Can Be Reconstituted In Vitro in the Absence of Phosphatase

Purified full-length recombinant Cdc25C (150 nM) was phosphorylated for 1 hr by various concentrations of recombinant p13 Suc1-Δ65-cyclin B1-Cdk1AF complexes in the presence of MgATP (500 μM). Data from nine experiments were scaled, pooled, and fitted to a Hill equation The Hill coefficient n_H was 2.3 with a 95% confidence interval of 1.9 to 2.7.

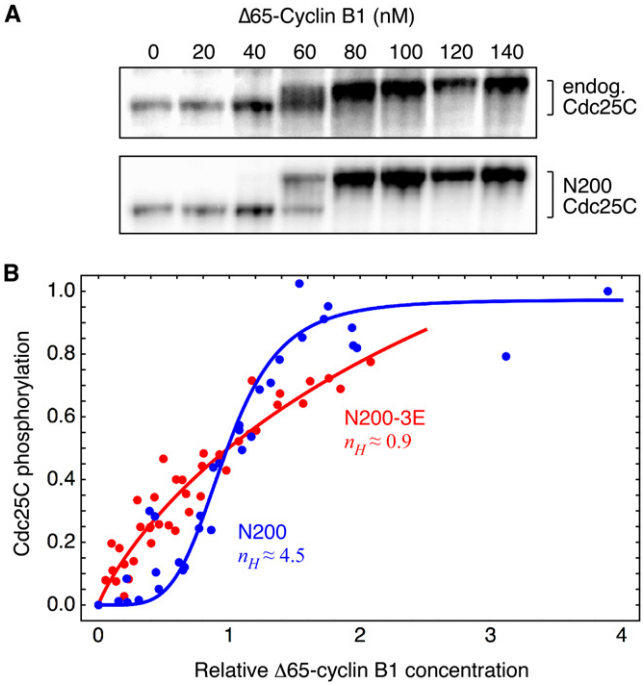

Figure 4. The Reconstituted Ultrasensitivity Is Decreased by Reducing the Number of Available Phosphosites

(A) Phosphorylation of a recombinant N-terminal fragment of Cdc25C (N200 Cdc25C) parallels that of endogenous Cdc25C. Interphase extracts were incubated with different concentrations ofΔ65-cyclin B1 and CDK1AF plus purified recombinant N200 Cdc25C. The hyperphosphorylation of endogenous Cdc25C and N200 Cdc25C were assessed by immunoblotting with Cdc25C antibody.

(B) Eliminating three conserved TP sites decreases ultrasensitivity. N200 Cdc25C or the same N-terminal fragment with three sites changed to glutamates (N200-3E, with T48E, T67E and T138E) were incubated with varying concentrations of recombinant p13 Suc1-Δ65-cyclin B1-Cdk1AF (complexes in the presence of MgATP [500 μM]) plus [γ-^{32}P]ATP. Phosphorylation of the N-terminal fragments was quantified by autoradiography. Scaled data were pooled and fitted to a three-parameter Hill equation. Hill coefficients were 4.5 (N200) with a 95% confidence interval of 2.7 to 6.3, and 0.9 (N200-3E) with a 95% confidence interval of 0.5 to 1.2.

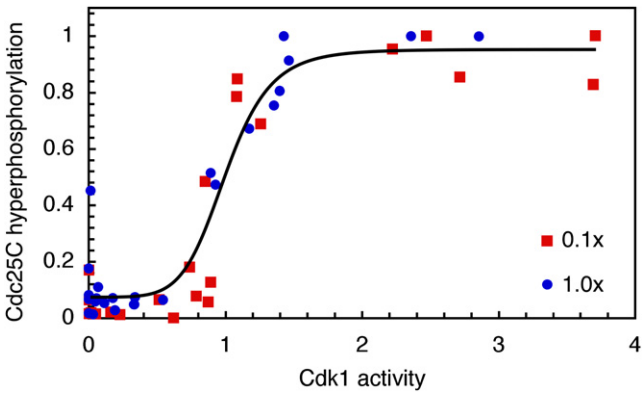

Figure 5. Ultrasensitivity in Extracts Does Not Decrease as Intermolecular Competition Is Reduced

Hyperphosphorylation of Cdc25C was carried out in normal extracts (blue circles) and extracts diluted 10-fold (red squares). Cdc25C was kept at endogenous levels (150 nM) in the diluted extract by addition of recombinant protein. Hyperphosphorylation was measured by immunoblotting and quantitation. Results from individual experiments were scaled to the fitted maximum levels of phosphorylation (*b*) and EC_{50} values (*K*), and combined. The line shown is a fit to all of the pooled scaled data. The Hill coefficient was estimated to be 8.

fragment of Cdc25C (N200) with nine SP/TP sites intact. In extracts, this N200-Cdc25C responds similarly to the full-length endogenous Cdc25C; as shown in Figure 4A, the EC_{50} for the gel shift of the fragment was indistinguishable from that of the full-length protein. Next, we constructed a mutant fragment with the three best-conserved SP/TP sites (T48, T67, T138) mutated to glutamates (N200-3E). Since the phosphorylated form of the N200-3E mutant was not shifted after phosphorylation (data not shown), we quantified the phosphorylation of N200 and N200-3E by ^{32}P radiolabeling rather than by immunoblotting. Radiolabel was found to be incorporated into both the shifted and nonshifted N200 bands, emphasizing that the nonshifted species is hypophosphorylated rather than nonphosphorylated, and to be incorporated to a lesser extent into the N200-3E band. As shown in Figure 4B, the incorporation of ^{32}P into N200 was ultrasensitive, with a Hill coefficient of 4.5. This was a slightly higher Hill coefficient than that seen for full-length Cdc25C (2.3; Figure 3), although with the scatter in both data sets, it is not clear that the difference is meaningful. N200-3E exhibited a hyperbolic response, with a Hill coefficient of 0.9 (95% CI of 0.5 to 1.2). This finding implies that multisite phosphorylation is responsible for the nonlinearity in the response of Cdc25C to Cdk1 in vitro.

Extrinsic Ultrasensitivity in the Cdc25C Response

Although substantial degrees of ultrasensitivity were seen in the reconstituted systems (Figures 3 and 4), the ultrasensitivity measured in extracts (Figure 1) was higher. A similar situation was reported for Wee1A: a substantially higher degree of ultrasensitivity was seen in extracts than was seen in vitro (Kim and Ferrell, 2007). In the case of Wee1A, it was hypothesized that the extrinsic ultrasensitivity was due to competition between Wee1A and either a stoichiometric inhibitor or a very-high-affinity Cdk1 substrate for access to Cdk1. In support of this hypothesis, it was found that diluting the extract, and hence diluting any competitors present, decreased the degree of ultrasensitivity observed in the Wee1A response (Kim and Ferrell, 2007). We reasoned that competition between Cdc25C and very-high-affinity Cdk1 binders might contribute to the ultrasensitivity seen in its response as well.

We tested this hypothesis by measuring the steady-state response of Cdc25C to Cdk1 in extracts as in Figure 1, but with two concentrations of extract and a constant concentration of Cdc25C. We added recombinant Cdc25C to both the 1:10 diluted and undiluted extracts to keep total Cdc25C concentrations in both extracts constant at approximately 150 nM. As shown in Figure 5, the response of the diluted extract was no less switch-like than that of the full-concentration extract. Thus, although the response of Cdc25C to Cdk1 activity is highly ultrasensitive in extracts, this ultrasensitivity is probably not due to intermolecular competition.

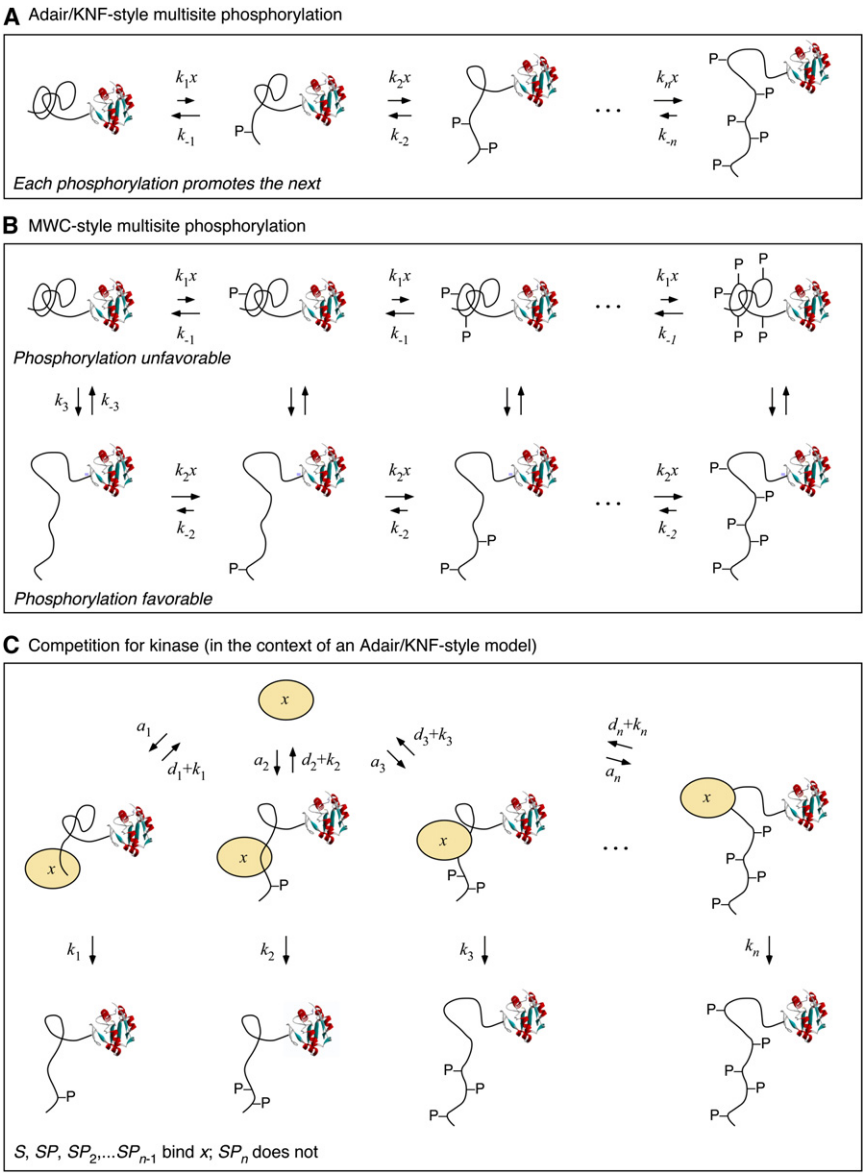

Figure 6. Schematic Views of Three Ways Multisite Phosphorylation Can Generate Ultrasensitivity

DISCUSSION

Here, we have shown that the hyperphosphorylation of Cdc25C in *Xenopus* egg extracts is a highly ultrasensitive function of the Cdk1 activity. The apparent Hill coefficient for the response is 11, an astronomical value for a Hill coefficient, and the Hill coefficient for Ser 287 dephosphorylation appeared to be even higher (Figure 1). Note that the exact values of the fitted Hill coefficients varied substantially from experiment to experiment and should probably be taken with a grain of salt. Nevertheless, there is no doubt that the responses of Cdc25C to Cdk1 are highly switch-like.

Some of the ultrasensitivity could be recapitulated in vitro with purified proteins under non-steady-state conditions (Figures 3 and 4). Essentially all of this intrinsic ultrasensitivity appeared to be due to multisite phosphorylation, as mutation of three conserved TP sites to nonphosphorylatable EP sites abolished the ultrasensitivity (Figure 4B). Thus, Cdc25C joins the yeast Sic1 and Ste5 proteins as examples of ultrasensitive responses generated by multisite phosphorylation (Nash et al., 2001; Strickfaden et al., 2007). Given how common multisite phosphorylation is (Holt et al., 2009; Moses et al., 2007), we suspect that there are many more examples to come. The additional extrinsic ultrasensitivity observed in extracts appeared not to be due to competition with stoichiometric inhibitors or higher affinity Cdk1 substrates (Figure 5). It is possible that other factors present in extracts but absent from the reconstituted system (e.g., Cdk1-regulated kinases like Plx1 and phosphatases like PP2A-B55δ and/or PP1 [Mochida et al., 2009; Wu et al., 2009]) contribute to this extrinsic ultrasensitivity.

Mechanisms through which Multisite Phosphorylation Can Generate Ultrasensitivity: Cooperativity and Competition

With as many as 14 SP/TP phosphorylation sites and other phosphorylation sites, as well, the number of specific mechanisms through which Cdc25C's ultrasensitive response might arise is enormous. For simplicity, we divide these mechanisms into two groups: Adair/Koshland-Nemethy-Filmer (Adair/KNF)-like mechanisms (Adair, 1925; Koshland et al., 1966) and Monod-Wyman-Changeux (MWC)-like mechanisms (Monod et al., 1965), and then also consider the additional effect of competition (Markevich et al., 2004; Thomson and Gunawardena, 2009).

For both an Adair/KNF-like mechanism and an MWC-like mechanism, we envision that Cdc25C undergoes a succession of phosphorylations by Cdk1 (designated *x* in Figure 6A). These phosphorylations may be random or ordered. Furthermore, we assume that the phosphorylations, the dephosphorylations, or both occur nonprocessively, and we assume that the concentration of kinase-substrate complexes is insignificant compared to the total concentration of the kinase.

For an Adair/KNF mechanism, we assume that each Cdc25C phosphorylation promotes the next, through some sort of priming mechanism or cooperativity between the sites (Figure 6A). The result is a sigmoidal dependence of the total

phosphorylation and the fraction of the Cdc25C in its most highly phosphorylated state on the concentration of the kinase *x*. If the cooperativity is very high, the effective Hill coefficient for the sigmoidal response (n_H) will approach the number of sites phosphorylated by kinase *x* (*n*). If no cooperativity is assumed, one obtains a slightly sigmoidal response.

For an MWC-like mechanism, we assume that Cdc25C can exist in two conformations: an inactive one where all of the sites are difficult to phosphorylate or easy to dephosphorylate (Figure 6B, top row) and an active one where phosphorylation is easy or dephosphorylation is difficult (Figure 6B, bottom row). This can result in a sigmoidal dependence of the fraction of Cdc25C in the active state, or of the fraction of Cdc25C in the most hyperphosphorylated form, again with a maximum effective Hill coefficient equal to the number of sites *n*.

In the competition-for-kinase mechanism, we assume that the concentrations of the kinase-substrate complexes are *not* insignificant (Figure 6C). Then, for a given total concentration of kinase *x*, as the concentration of free *x* increases, the fraction of Cdc25C in the kinase-binding hypophosphorylated states decreases, which frees up more *x*, which further decreases the amount of hypophosphorylated Cdc25C present, and so on. The result is the equivalent of positive feedback, with *x* promoting the freeing up of more *x*. Under the proper circumstances, this positive feedback can lead to bistability or multistability (Markevich et al., 2004; Thomson and Gunawardena, 2009). However, even when the strength of the feedback is insufficient to yield multistability, it can raise the ultrasensitivity of the system's response beyond the $n_H = n$ limit.

Given that there are at least five phosphorylation sites in the N terminus of Cdc25C, 14 total SP/TP sites, and additional other possible sites, either an Adair/KNF model or an MWC model can easily account for the intrinsic ultrasensitivity (n_H = 2 to 4.5) observed for Cdc25C. The higher degree of ultrasensitivity seen in extracts ($n_H \approx 11$) suggests that the total number of phosphorylation sites relevant is higher, the competition-for-kinase mechanism applies, or the relevant phosphatases are regulated in a switch-like fashion.

Can the Observed Cdc25C and Wee1 Response Functions Account for the Bistable Mitotic Trigger?

Given that we now have response functions for the regulation of Cdc25C (the present work) and Wee1A (Kim and Ferrell, 2007) by Cdk1, how well can we account for the observed bistability in Cdk1 regulation in extracts (Pomerening et al., 2003; Sha et al., 2003)?

One way to approach this question is through the rate-balance formalism. We use the observed response functions to calculate curves for the rates of Cdk1 activation and inactivation as functions of the activity of Cdk1. If the activation and inactivation curves intersect once, the system is monostable. If they intersect three times, the system is bistable, with the middle intersection point representing an unstable threshold. Based on the experimentally observed behavior of the Cdk1 system (Figure 7A), the rate-balance analysis should yield monostability at low cyclin concentrations (with the Cdk1 in a low activity state), monostability at high cyclin concentrations (with the Cdk1 in a high activity state), and bistability in between.

The reactions included in the model are shown schematically in Figure 7B. We assume mass action kinetics for the activation and inactivation of cyclin-Cdk1:

$$Activation\ \ rate = k_{act}(CycCdk1_{tot} - CycCdk1^*)\cdot Cdc25C^*, \quad (1)$$

where *CycCdk1** denotes the concentration of active cyclin B1-Cdk1 complexes and *Cdc25C** denotes the concentration of active Cdc25C. We assume that cyclin binds rapidly and with high affinity to Cdk1 and that Cdk1 is in excess (in *Xenopus* extracts the concentration of Cdk1 is approximately 200 nM (Pomerening et al., 2003), whereas the cyclin concentrations under consideration are less than 100 nM). Thus, $CycCdk1_{tot} = Cyclin_{tot}$ and

$$Activation\ \ rate = k_{act}(Cyclin_{tot} - CycCdk1^*)\cdot Cdc25C^*. \quad (2)$$

For simplicity, we also assume that the regulation of Cdc25C by Cdk1 is rapid relative to the regulation of Cdk1 by Cdc25C. This assumption allows us to reduce Equation 2 to an equation with only one time-dependent variable (*CycCdk1**). Note though that even without this assumption, one can delineate the steady states of the system (and Equation 6, which relates the total concentration of cyclin to the possible steady-state levels of Cdk1 activity still holds), although the stability of the steady states is somewhat less easy to ascertain.

The hyperphosphorylation of Cdc25C as a function of Cdk1 is well approximated by a Hill function, and we assume that the dependence of Cdc25C activity on Cdk1 activity is as well. It follows that

$$Activation\ \ rate = k_{Cdc25C}(Cyclin_{tot} - CycCdk1^*) \times \left(bkgd_{Cdc25C} + \frac{CycCdk1^{*nCdc25C}}{EC50_{Cdc25C}^{nCdc25C} + CycCdk1^{*nCdc25C}}\right), \quad (3)$$

where the new rate constant k_{Cdc25C} is introduced to account for the fact that we have replaced a concentration (*Cdc25C**) with a dimensionless quantity.

We can carry out a similar analysis for the rate of inactivation of Cdk1. By the law of mass action, the inactivation rate should be proportional to the concentrations of active cyclin B1-Cdk1 and active Wee1A:

$$Inactivation\ \ rate = k_{inact} CycCdk1^*\cdot Wee1A^*. \quad (4)$$

Assuming (as we did for Cdc25C) that the regulation of Wee1A by Cdk1 is rapid, and taking the steady-state activity of Wee1A to be given by an inhibitory Hill function of the form $a + K^n/K^n + x^n$, it follows that

$$Inactivation\ \ rate = k_{Wee1A} CycCdk1^* \times \left(bkgd_{Wee1A} + \frac{EC50_{wee1A}^{nWee1A}}{EC50_{wee1A}^{nWee1A} + CycCdk1^{*nWee1A}}\right). \quad (5)$$

At steady state, the rate of Cdk1 activation equals the rate of Cdk1 inactivation. Combining Equations 3 and 5, we can

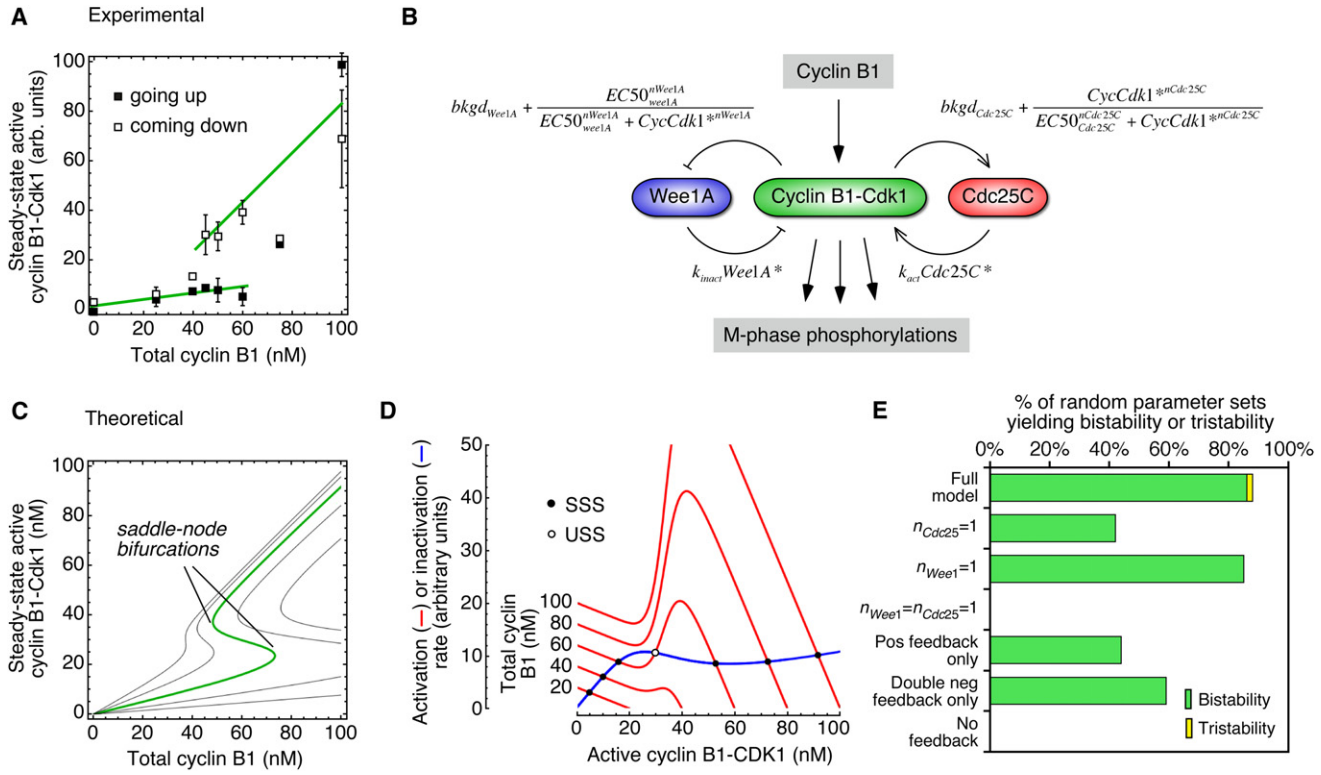

Figure 7. A Model Based on the Experimentally Observed Response Functions for Wee1 and Cdc25C Accounts for the Bistability of the Mitotic Trigger

(A) Experimental data for the hysteretic response of Cdk1 to recombinantΔ65-cyclin B1 in *Xenopus* egg extracts. Data are taken from a previous publication (Pomerening et al., 2003).

(B) Schematic view of the regulation of cyclin B1-Cdk1 activity by cyclin B1, Wee1A, and Cdc25C.

(C) Theoretical steady-state responses based on Equation 6, for five assumed values of k_{Wee1A}/k_{Cdc25C} (left to right: 0.125, 0.25, 0.5 [green], 1, and 2).

(D) Rate-balance plots. The calculated rates of Cdk1 activation (red curves) and inactivation (blue curve) as a function of the concentration of active cyclin B1-Cdk1. The five red curves correspond to five assumed total cyclin concentrations. The ratio k_{Wee1A}/k_{Cdc25C} is assumed to be 0.5.

(E) Robustness of the bistable response. For the full model and various modified models, we calculated response curves for 100 randomly generated parameter sets. The ranges of the parameters were as follows:

$bkgd_{Cdc25C}$ = 0 to 0.4 (experimental estimate = 0.2)

$bkgd_{Wee1A}$ = 0 to 0.4 (experimental estimate = 0.2)

$EC_{50Cdc25C}$ = 20 to 80 nM (experimental estimate = 30 nM)

$EC_{50Wee1A}$ = 20 to 80 nM (experimental estimate = 35 nM)

n_{Cdc25C} = 5 to 15 (experimental estimate = 11)

n_{Wee1A} = 1.5 to 8 (experimental estimate = 3.5)

k_{Wee1A}/k_{Cdc25C} = 0 to 1.5

Random parameter sets were generated and curves were plotted with Mathematica 6.0.3.

See also Figures S1 and S2.

derive an equation for the relationship between the total cyclin concentration and the activity of cyclin B1-Cdk1 at steady state:

$$Cyclin_{tot} = \frac{CycCdk1^{*}\left(\left(bkgd_{Cdc25C} + \frac{CycCdk1^{*nCdc25C}}{EC50_{Cdc25C}^{nCdc25C} + CycCdk1^{*nCdc25C}}\right) + \frac{k_{Wee1A}}{k_{Cdc25C}}\left(bkgd_{Wee1A} + \frac{EC50_{Wee1A}^{nWee1A}}{EC50_{Wee1A}^{nWee1A} + CycCdk1^{*nWee1A}}\right)\right)}{bkgd_{Cdc25C} + \frac{CycCdk1^{*nCdc25C}}{EC50_{Cdc25C}^{nCdc25C} + CycCdk1^{*nCdc25C}}}. \quad (6)$$

Similarly, one can derive an equation for the relationship between the total cyclin concentration and the activity of cyclin B1-Cdk1 at steady state under the assumption that Cdk1 activation and inactivation are described by Michaelis-Menten kinetics rather than mass action kinetics (see the Supplemental Results and Figure S1 available online).

Parameterizing the Steady-State Response Function

We now have experimental estimates for almost all of the parameters that enter into Equation 6. From the present work, the Hill

coefficient n_{Cdc25C} was found to be approximately 11, and the Hill coefficient for Wee1A inactivation was previously reported to be approximately 3.5 (Kim and Ferrell, 2007). The constant $EC50_{Cdc25C}$, which is the concentration of cyclin at which Cdc25C hyperphosphorylation is half-maximal, varied from 30 to 60 nM for various cyclin preparations; here, we will take it to be 35 nM and, based on the results in Figure 2, will take $EC50_{Wee1A}$ to be slightly lower, 30 nM. Previous work suggests that the dimensionless basal activities of Cdc25C and Wee1A ($bkgd_{Cdc25C}$ and $bkgd_{Wee1A}$) are approximately 0.2 (Izumi et al., 1992; Kim et al., 2005; Kumagai and Dunphy, 1992; Solomon et al., 1990). The only unmeasured parameters in Equation 6 are k_{Wee1A}, rate constant for the inactivation of Cdk1 by active Wee1A, and k_{Cdc25C}, the rate constant for the activation of Cdk1 by active Cdc25C, and these parameters enter into Equation 6 only as their ratio.

We can now plot the steady-state activity of Cdk1 as a function of the total cyclin concentration for various assumed values of the ratio k_{Wee1A}/k_{Cdc25C}. As shown in Figure 7C, Equation 6 defines a family of S-shaped curves, and an assumed ratio of $k_{Wee1A}/k_{Cdc25C} = 0.5$ yields a curve whose overall shape and absolute thresholds closely approximate the experimentally observed hysteretic response (Figure 7A).

We can also plot the rate of Cdk1 activation (Equation 3) and inactivation (Equation 5) as functions of the cyclin concentration, to see how the bistability of the modeled system arises. At low cyclin B1 concentrations, the activation and inactivation curves have one intersection point and the system is monostable, with low, interphase-like concentrations of active cyclin B1-Cdk1 (Figure 7D). At around 40 nM cyclin B1, the positive feedback in the Cdc25C loop begins to produce a bump in the activation rate curve, and just above 40 nM cyclin B1, the system goes through a saddle-node bifurcation, with a new high-activity steady state and new threshold appearing out of thin air. Over a range of ~45–75 nM cyclin B1, the system is bistable (Figure 7D). Above ~75 nM cyclin B1, the low activity steady-state and the threshold annihilate each other in a second saddle-node bifurcation, and the system once again becomes monostable (Figure 7D), this time with a high, mitotic level of Cdk1 activity. Thus, the model suggests that the transition from interphase into mitosis is the result of the traversal of one saddle-node bifurcation in the Cdk1/Cdc25C/Wee1A system. The other saddle-node bifurcation could contribute to mitotic exit.

Which Features of the Model Are Important for Robust Bistability?

To see how sensitive the steady-state response curve was to the exact values chosen for the six experimentally determined parameters ($bkgd_{Cdc25C}$, $bkgd_{Wee1A}$, $EC50_{Cdc25C}$, $EC50_{Wee1A}$, n_{Cdc25C}, and n_{Wee1A}) and the fitted value of k_{Wee1A}/k_{Cdc25C}, we randomized all of these parameters over reasonable ranges and recalculated the response curve for 100 random parameter sets. We obtained S-shaped bistable response curves 86% of the time, monostable response curves 12% of the time, and tristable responses 2% of the time (Figure 7E). Thus, the bistable response was robust with respect to parameter variation.

To see what aspects of the model were important for the robust bistability, we eliminated the assumed ultrasensitive response functions and the feedback loops one at a time and again assessed the calculated response curves using 100 random parameter sets. Elimination of Cdc25C's ultrasensitivity decreased the robustness of the bistability, and elimination of the ultrasensitivity from both Wee1A and Cdc25C decreased it much further (Figure 7E). (Within the assumed parameter ranges, it is possible to achieve a bistable response without assuming ultrasensitivity in the responses in either Wee1A or Cdc25C, but the probability is low; see Figure S2). Individual elimination of either the positive feedback loop or the double-negative feedback loop compromised the robustness of the bistable response, and elimination of both made bistability impossible (Figure 7E). Thus, the ultrasensitivity of the Wee1A and Cdc25C response functions and the mirror-image, positive feedback plus double-negative feedback topology of the circuit all contribute to the robustness of the bistability.

In summary, these findings show that the mitotic trigger, a complex multi-feedback loop system, can be understood in terms of a simple model with only one time-dependent variable (the concentration of active cyclin B1-Cdk1). Our findings hearken back to the earliest, simplest models of the bistable trigger proposed by Novak and Tyson (1993b); although the details of our model differ from those of theirs, the underlying concepts are the same.

One of the goals of systems biology is to provide a simpler, albeit more abstract, understanding of complex biological phenomena. The mitotic trigger provides a good example of how quantitative experimentation and computational modeling can combine to yield this type of understanding. The close agreement between our simple mathematical model of the steady states of the process and the experimentally observed response data argues that saddle-node bifurcations in the dynamics of the system allow these continuously variable, reversible enzymatic processes to collectively generate a discontinuous, hysteretic steady-state response.

EXPERIMENTAL PROCEDURES

Xenopus Extract Preparation

Interphase egg extracts supplemented with an ATP regenerating system and cycloheximide (100 μg/ml) were prepared as described (Murray, 1991; Smythe and Newport, 1991) and treated with nondegradable *Xenopus*Δ65-cyclin B1 and noninactivatable Cdk1AF to produce extracts with various levels of Cdk1 activity. Demembranated sperm chromatin was added at 500/μl to monitor mitotic progression. Frozen extract samples (the equivalent of 0.2 μl extract) were used for histone H1 kinase assay as described (Murray, 1991). The ^{32}P-labeled histone was detected and quantified by SDS gel electrophoresis followed by blotting and imaging by phosphorimager. For Cdc25C blotting, the equivalent of 0.5 μl extract was detected and quantified by SDS gel electrophoresis and immunoblotting (1:1000). The slower- and faster-migrating bands were quantified by GelDoc (Bio-Rad, Hercules, CA).

Recombinant Proteins

His-tagged wild-type *Xenopus* Cdc25C was purified from insect cells after baculovirus infection. Sf9 cells were pelleted and resuspended in lysis buffer (10 mM HEPES, 150 mM NaCl, 0.5% Triton X-100, 5 mM 2-mercaptoethanol [pH 8.0]) (Kumagai and Dunphy, 1997). The lysate was subjected to sonication and then centrifuged at 50,000 g for 30 min. The resulting supernatant was bound to Talon cobalt resin and washed with 20 ml wash buffer (10 mM HEPES, 400 mM NaCl, 0.5% Triton X-100, 5 mM 2-mercaptoethanol [pH 8.0]) followed by 6 ml HBS (10 mM HEPES, 150 mM NaCl). Protein was then eluted in 0.5 ml fractions with 10 ml elution buffer (10 mM HEPES,

150 mM NaCl, 150 mM imidazole, 5 mM 2-mercaptoethanol [pH 8.0]). Fractions containing Cdc25C were pooled and dialyzed into final solution (10 mM HEPES, 150 mM NaCl, 5 mM 2-mercaptoethanol [pH 8.0]).

Purification of Complexed Cdk1AF/Δ65Cyclin B1/p13 Suc1

Flag-tagged *Xenopus* Δ65-cyclin B1 was purified from baculovirus. Sf9 cells were pelleted by centrifugation, and the resulting pellet was resuspended in a hypotonic lysis buffer (10 mM HEPES, 10 mM NaCl, 1 mM EDTA) with the addition of protease inhibitors (10 μg/ml chymotrypsin, pepstatin and leupeptin). The lysate subjected to sonication and then centrifuged at 50,000 g for 30 min. The resulting supernatant was bound to FLAG resin for 16 hr. The Cdk1 pellet was then lysed in 50 mM Tris-HCl, 150 mM NaCl, 1 mM EDTA, 10 mM 2-mercaptoethanol, 0.5 mM ATP, 10 mM $MgCl_2$, 0.1% Nonidet P-40, 10 μg/ml chymotrypsin, 10 μg/ml pepstatin, and 10 μg/ml leupeptin (pH 7.4). The lysate was then centrifuged, and the supernatant was mixed with the FLAG resin with bound Δ65-cyclin B1. The resin and lysate were agitated together at 4°C for 4 hr, and then washed three times with KBD buffer (20 mM HEPES, 150 mM NaCl, 5 mM $MgCl_2$, 10% sucrose, 0.1% Nonidet P-40 [pH 7.7]) and once with KB (20 mM HEPES, 150 mM NaCl, 5 mM $MgCl_2$, 10% sucrose [pH 7.7]). The complex was eluted from the resin by agitation for 2 hr with KB containing FLAG peptide and 1 mM DTT.

GST-Suc1 was expressed in bacteria. Protein expression was induced with 0.3 mM IPTG for 4 hr, after which the cells were pelleted and frozen. After thawing, the cells were lysed with lysozyme followed by sonication. The lysate was then centrifuged at 50,000 g for 30 min. The resulting supernatant was bound to glutathione resin and washed with KBD buffer (20 mM HEPES, 150 mM NaCl, 5 mM $MgCl_2$, 10% sucrose, 0.1% Nonidet P-40 [pH 7.7]) and once with KB (20 mM HEPES, 150 mM NaCl, 5 mM $MgCl_2$, 10% sucrose [pH 7.7]). The resin was then combined with the eluted Δ65-cyclin B-Cdk1 and agitated for 4 hr at 4°C. The resin was then washed with KBD buffer and once with KB and then eluted in KB buffer containing 10 mM glutathione. Glycerol was added to 5%, and the protein was stored at −70°.

Cdc25C Phosphorylation In Vitro

Cdc25C phosphorylation in vitro was carried out in a buffer containing 50 mM Tris-Cl (pH 7.5), 10 mM $MgCl_2$, 0.3 mM ATP, 2 mM dithiothreitol, 0.01% Brij35, and 1 mM EGTA. Cdc25C (150 nM) was incubated with 0–120 nM Cdk1/cyclin B1/Suc1 complex for 2 hr, and hyperphosphorylation was assessed by immunoblotting. Control experiments showed that Cdk1 did not lose activity during the 2 hr incubation. For radiolabeling experiments, N200 Cdc25C or the same N-terminal fragment with three sites changed to glutamates (N200-3E, with T48E, T67E, and T138E) were incubated with varying concentrations of recombinant p13 Suc1-Δ65-cyclin B1-Cdk1AF (complexes in the presence of MgATP [0.5 mM]) plus [γ-^{32}P]ATP. Phosphorylation of the N-terminal fragments was quantified by autoradiography.

Curve Fitting

Steady-state response data were typically fitted to a three-parameter Hill equation,

$$y = \frac{bx^{n_H}}{K^{n_H} + x^{n_H}},$$

where y was the Cdc25C hyperphosphorylation and x was the Cdk1 activity, if the background level of response appeared to be zero. Alternatively, if the background level of response was non-zero, a four-parameter Hill equation was used:

$$y = a + \frac{bx^{n_H}}{K^{n_H} + x^{n_H}}.$$

To combine data from different experiments, we first scaled the Cdk1 activities (x values) for each individual experiment to the fitted K value for that experiment, and then pooled the scaled data and re-fit it to a Hill function to estimate the overall Hill coefficient. The rationale for this scaling is that the best fit to two pooled, unscaled, ultrasensitive data sets is generally less ultrasensitive—sometimes much less ultrasensitive—than the fits to the individual data sets are, if there is variability from experiment to experiment in terms of potency of the cyclin B1-Cdk1AF preparations or in the extract's responsiveness. Scaling avoids this problem of systematically underestimating the ultrasensitivity of the response.

SUPPLEMENTAL INFORMATION

Supplemental Information includes Supplemental Results and two figures and can be found with this article online at doi:10.1016/j.molcel.2011.01.012.

ACKNOWLEDGMENTS

We thank Bill Dunphy and Akiko Kumagai for generously sharing their Cdc25C baculovirus, Joan Ruderman for the generous gift of the pS287 Cdc25C antibody, Zach Serber for help and advice, and Joe Pomerening, Silvia Santos, and the rest of the Ferrell lab for comments on the manuscript. This work was supported by grants from the National Institutes of Health (GM046383 and CA009302).

Received: September 11, 2009
Revised: July 29, 2010
Accepted: December 22, 2010
Published: February 3, 2011

REFERENCES

Adair, G.S. (1925). The hemoglobin system. VI. The oxygen dissociation curve of hemoglobin. J. Biol. Chem. *63*, 529–545.

Bonnet, J., Coopman, P., and Morris, M.C. (2008). Characterization of centrosomal localization and dynamics of Cdc25C phosphatase in mitosis. Cell Cycle *7*, 1991–1998.

Booher, R.N., Holman, P.S., and Fattaey, A. (1997). Human Myt1 is a cell cycle-regulated kinase that inhibits Cdc2 but not Cdk2 activity. J. Biol. Chem. *272*, 22300–22306.

Deibler, R.W., and Kirschner, M.W. (2010). Quantitative reconstitution of mitotic CDK1 activation in somatic cell extracts. Mol. Cell *37*, 753–767.

Elia, A.E., Cantley, L.C., and Yaffe, M.B. (2003). Proteomic screen finds pSer/pThr-binding domain localizing Plk1 to mitotic substrates. Science *299*, 1228–1231.

Fattaey, A., and Booher, R.N. (1997). Myt1: a Wee1-type kinase that phosphorylates Cdc2 on residue Thr14. Prog. Cell Cycle Res. *3*, 233–240.

Fauman, E.B., Cogswell, J.P., Lovejoy, B., Rocque, W.J., Holmes, W., Montana, V.G., Piwnica-Worms, H., Rink, M.J., and Saper, M.A. (1998). Crystal structure of the catalytic domain of the human cell cycle control phosphatase, Cdc25A. Cell *93*, 617–625.

Ferguson, A.M., White, L.S., Donovan, P.J., and Piwnica-Worms, H. (2005). Normal cell cycle and checkpoint responses in mice and cells lacking Cdc25B and Cdc25C protein phosphatases. Mol. Cell. Biol. *25*, 2853–2860.

Ferrell, J.E., Jr. (2008). Feedback regulation of opposing enzymes generates robust, all-or-none bistable responses. Curr. Biol. *18*, R244–R245.

Ferrell, J.E., Jr., and Xiong, W. (2001). Bistability in cell signaling: How to make continuous processes discontinuous, and reversible processes irreversible. Chaos *11*, 227–236.

Furnari, B., Rhind, N., and Russell, P. (1997). Cdc25 mitotic inducer targeted by chk1 DNA damage checkpoint kinase. Science *277*, 1495–1497.

Heald, R., McLoughlin, M., and McKeon, F. (1993). Human wee1 maintains mitotic timing by protecting the nucleus from cytoplasmically activated Cdc2 kinase. Cell *74*, 463–474.

Hoffmann, I., Clarke, P.R., Marcote, M.J., Karsenti, E., and Draetta, G. (1993). Phosphorylation and activation of human cdc25-C by cdc2—cyclin B and its involvement in the self-amplification of MPF at mitosis. EMBO J. *12*, 53–63.

Holt, L.J., Tuch, B.B., Villén, J., Johnson, A.D., Gygi, S.P., and Morgan, D.O. (2009). Global analysis of Cdk1 substrate phosphorylation sites provides insights into evolution. Science *325*, 1682–1686.

Izumi, T., and Maller, J.L. (1993). Elimination of cdc2 phosphorylation sites in the cdc25 phosphatase blocks initiation of M-phase. Mol. Biol. Cell *4*, 1337–1350.

Izumi, T., Walker, D.H., and Maller, J.L. (1992). Periodic changes in phosphorylation of the Xenopus cdc25 phosphatase regulate its activity. Mol. Biol. Cell *3*, 927–939.

Kim, S.Y., and Ferrell, J.E., Jr. (2007). Substrate competition as a source of ultrasensitivity in the inactivation of Wee1. Cell *128*, 1133–1145.

Kim, S.Y., Song, E.J., Lee, K.J., and Ferrell, J.E., Jr. (2005). Multisite M-phase phosphorylation of Xenopus Wee1A. Mol. Cell. Biol. *25*, 10580–10590.

Koshland, D.E., Jr., Némethy, G., and Filmer, D. (1966). Comparison of experimental binding data and theoretical models in proteins containing subunits. Biochemistry *5*, 365–385.

Kumagai, A., and Dunphy, W.G. (1992). Regulation of the cdc25 protein during the cell cycle in Xenopus extracts. Cell *70*, 139–151.

Kumagai, A., and Dunphy, W.G. (1996). Purification and molecular cloning of Plx1, a Cdc25-regulatory kinase from Xenopus egg extracts. Science *273*, 1377–1380.

Kumagai, A., and Dunphy, W.G. (1997). Regulation of Xenopus Cdc25 protein. Methods Enzymol. *283*, 564–571.

Kumagai, A., and Dunphy, W.G. (1999). Binding of 14-3-3 proteins and nuclear export control the intracellular localization of the mitotic inducer Cdc25. Genes Dev. *13*, 1067–1072.

Lee, G., White, L.S., Hurov, K.E., Stappenbeck, T.S., and Piwnica-Worms, H. (2009). Response of small intestinal epithelial cells to acute disruption of cell division through CDC25 deletion. Proc. Natl. Acad. Sci. USA *106*, 4701–4706.

Liu, F., Stanton, J.J., Wu, Z., and Piwnica-Worms, H. (1997). The human Myt1 kinase preferentially phosphorylates Cdc2 on threonine 14 and localizes to the endoplasmic reticulum and Golgi complex. Mol. Cell. Biol. *17*, 571–583.

Lopez-Girona, A., Furnari, B., Mondesert, O., and Russell, P. (1999). Nuclear localization of Cdc25 is regulated by DNA damage and a 14-3-3 protein. Nature *397*, 172–175.

Lopez-Girona, A., Kanoh, J., and Russell, P. (2001). Nuclear exclusion of Cdc25 is not required for the DNA damage checkpoint in fission yeast. Curr. Biol. *11*, 50–54.

Manke, I.A., Nguyen, A., Lim, D., Stewart, M.Q., Elia, A.E., and Yaffe, M.B. (2005). MAPKAP kinase-2 is a cell cycle checkpoint kinase that regulates the G2/M transition and S phase progression in response to UV irradiation. Mol. Cell *17*, 37–48.

Markevich, N.I., Hoek, J.B., and Kholodenko, B.N. (2004). Signaling switches and bistability arising from multisite phosphorylation in protein kinase cascades. J. Cell Biol. *164*, 353–359.

Matsuoka, S., Huang, M., and Elledge, S.J. (1998). Linkage of ATM to cell cycle regulation by the Chk2 protein kinase. Science *282*, 1893–1897.

Matsuoka, S., Rotman, G., Ogawa, A., Shiloh, Y., Tamai, K., and Elledge, S.J. (2000). Ataxia telangiectasia-mutated phosphorylates Chk2 in vivo and in vitro. Proc. Natl. Acad. Sci. USA *97*, 10389–10394.

McGowan, C.H., and Russell, P. (1993). Human Wee1 kinase inhibits cell division by phosphorylating p34cdc2 exclusively on Tyr15. EMBO J. *12*, 75–85.

McGowan, C.H., and Russell, P. (1995). Cell cycle regulation of human WEE1. EMBO J. *14*, 2166–2175.

Millar, J.B., McGowan, C.H., Lenaers, G., Jones, R., and Russell, P. (1991). p80cdc25 mitotic inducer is the tyrosine phosphatase that activates p34cdc2 kinase in fission yeast. EMBO J. *10*, 4301–4309.

Mochida, S., Ikeo, S., Gannon, J., and Hunt, T. (2009). Regulated activity of PP2A-B55 delta is crucial for controlling entry into and exit from mitosis in Xenopus egg extracts. EMBO J. *28*, 2777–2785.

Monod, J., Wyman, J., and Changeux, J.P. (1965). On the nature of allosteric transitions: a plausible model. J. Mol. Biol. *12*, 88–118.

Morgan, D.O. (2007). The Cell Cycle: Principles of Control (London, UK: New Science Press Ltd.).

Moses, A.M., Hériché, J.K., and Durbin, R. (2007). Clustering of phosphorylation site recognition motifs can be exploited to predict the targets of cyclin-dependent kinase. Genome Biol. *8*, R23.

Mueller, P.R., Coleman, T.R., and Dunphy, W.G. (1995a). Cell cycle regulation of a Xenopus Wee1-like kinase. Mol. Biol. Cell *6*, 119–134.

Mueller, P.R., Coleman, T.R., Kumagai, A., and Dunphy, W.G. (1995b). Myt1: a membrane-associated inhibitory kinase that phosphorylates Cdc2 on both threonine-14 and tyrosine-15. Science *270*, 86–90.

Murray, A.W. (1991). Cell cycle extracts. Methods Cell Biol. *36*, 581–605.

Nash, P., Tang, X., Orlicky, S., Chen, Q., Gertler, F.B., Mendenhall, M.D., Sicheri, F., Pawson, T., and Tyers, M. (2001). Multisite phosphorylation of a CDK inhibitor sets a threshold for the onset of DNA replication. Nature *414*, 514–521.

Novak, B., and Tyson, J.J. (1993a). Modeling the cell division cycle: M-phase trigger, oscillations, and size control. J. Theor. Biol. *165*, 101–134.

Novak, B., and Tyson, J.J. (1993b). Numerical analysis of a comprehensive model of M-phase control in Xenopus oocyte extracts and intact embryos. J. Cell Sci. *106*, 1153–1168.

Palmer, A., Gavin, A.C., and Nebreda, A.R. (1998). A link between MAP kinase and p34(^{cdc2})/cyclin B during oocyte maturation: p90(^{rsk}) phosphorylates and inactivates the p34(^{cdc2}) inhibitory kinase Myt1. EMBO J. *17*, 5037–5047.

Parker, L.L., and Piwnica-Worms, H. (1992). Inactivation of the p34cdc2-cyclin B complex by the human WEE1 tyrosine kinase. Science *257*, 1955–1957.

Peng, C.Y., Graves, P.R., Ogg, S., Thoma, R.S., Byrnes, M.J., 3rd, Wu, Z., Stephenson, M.T., and Piwnica-Worms, H. (1998). C-TAK1 protein kinase phosphorylates human Cdc25C on serine 216 and promotes 14-3-3 protein binding. Cell Growth Differ. *9*, 197–208.

Pomerening, J.R., Sontag, E.D., and Ferrell, J.E., Jr. (2003). Building a cell cycle oscillator: hysteresis and bistability in the activation of Cdc2. Nat. Cell Biol. *5*, 346–351.

Pomerening, J.R., Kim, S.Y., and Ferrell, J.E., Jr. (2005). Systems-level dissection of the cell-cycle oscillator: bypassing positive feedback produces damped oscillations. Cell *122*, 565–578.

Pomerening, J.R., Ubersax, J.A., and Ferrell, J.E., Jr. (2008). Rapid cycling and precocious termination of G1 phase in cells expressing CDK1AF. Mol. Biol. Cell *19*, 3426–3441.

Sanchez, Y., Wong, C., Thoma, R.S., Richman, R., Wu, Z., Piwnica-Worms, H., and Elledge, S.J. (1997). Conservation of the Chk1 checkpoint pathway in mammals: linkage of DNA damage to Cdk regulation through Cdc25. Science *277*, 1497–1501.

Sha, W., Moore, J., Chen, K., Lassaletta, A.D., Yi, C.S., Tyson, J.J., and Sible, J.C. (2003). Hysteresis drives cell-cycle transitions in Xenopus laevis egg extracts. Proc. Natl. Acad. Sci. USA *100*, 975–980.

Shen, M., Stukenberg, P.T., Kirschner, M.W., and Lu, K.P. (1998). The essential mitotic peptidyl-prolyl isomerase Pin1 binds and regulates mitosis-specific phosphoproteins. Genes Dev. *12*, 706–720.

Smythe, C., and Newport, J.W. (1991). Systems for the study of nuclear assembly, DNA replication, and nuclear breakdown in Xenopus laevis egg extracts. Methods Cell Biol. *35*, 449–468.

Solomon, M.J., Glotzer, M., Lee, T.H., Philippe, M., and Kirschner, M.W. (1990). Cyclin activation of p34^{cdc2}. Cell *63*, 1013–1024.

Strausfeld, U., Labbé, J.C., Fesquet, D., Cavadore, J.C., Picard, A., Sadhu, K., Russell, P., and Dorée, M. (1991). Dephosphorylation and activation of a p34cdc2/cyclin B complex in vitro by human CDC25 protein. Nature *351*, 242–245.

Strickfaden, S.C., Winters, M.J., Ben-Ari, G., Lamson, R.E., Tyers, M., and Pryciak, P.M. (2007). A mechanism for cell-cycle regulation of MAP kinase signaling in a yeast differentiation pathway. Cell *128*, 519–531.

Stukenberg, P.T., and Kirschner, M.W. (2001). Pin1 acts catalytically to promote a conformational change in Cdc25. Mol. Cell *7*, 1071–1083.

Thomson, M., and Gunawardena, J. (2009). Unlimited multistability in multisite phosphorylation systems. Nature *460*, 274–277.

Thron, C.D. (1994). Theoretical dynamics of the cyclin B-MPF system: a possible role for p13suc1. Biosystems *32*, 97–109.

Thron, C.D. (1996). A model for a bistable biochemical trigger of mitosis. Biophys. Chem. *57*, 239–251.

Toyoshima-Morimoto, F., Taniguchi, E., and Nishida, E. (2002). Plk1 promotes nuclear translocation of human Cdc25C during prophase. EMBO Rep. *3*, 341–348.

Wang, R., He, G., Nelman-Gonzalez, M., Ashorn, C.L., Gallick, G.E., Stukenberg, P.T., Kirschner, M.W., and Kuang, J. (2007). Regulation of Cdc25C by ERK-MAP kinases during the G2/M transition. Cell *128*, 1119–1132.

Wu, J.Q., Guo, J.Y., Tang, W., Yang, C.S., Freel, C.D., Chen, C., Nairn, A.C., and Kornbluth, S. (2009). PP1-mediated dephosphorylation of phosphoproteins at mitotic exit is controlled by inhibitor-1 and PP1 phosphorylation. Nat. Cell Biol. *11*, 644–651.

Zhou, X.Z., Kops, O., Werner, A., Lu, P.J., Shen, M., Stoller, G., Küllertz, G., Stark, M., Fischer, G., and Lu, K.P. (2000). Pin1-dependent prolyl isomerization regulates dephosphorylation of Cdc25C and tau proteins. Mol. Cell *6*, 873–883.